IEC-185

submitted to J. Nucl. Technol.

Validity of DWBA Calculations for Neutron Inelastic Scattering from Molybdenum Isotopes

Toshihiko KAWANO*, Yukinobu WATANABE*
and Masayoshi KAWAI**

**Department of Advanced Energy Engineering Science, Kyushu University*
***High Energy Accelerator Research Organization*

Neutron inelastic scattering cross sections for molybdenum isotopes are calculated with the DWBA and the coupled-channels methods. Anomalous enhancement of the DWBA cross sections near the threshold energy appears when the adopted optical potential has a shallow imaginary part. Calculations with some simplified optical potentials indicate that the enhancement can be related with the p-wave strength, and it is found that the problem comes from the optical potential used.

When an adopted optical potential to the DWBA calculation is physically reasonable, differences between the calculated cross sections with the DWBA and those with the coupled-channels theory are small. Experimental data of ^{92}Mo, ^{98}Mo and ^{100}Mo are well reproduced by the calculated cross sections with the DWBA and the Hauser-Feshbach-Moldauer statistical model, and it is concluded that the DWBA is an appropriate method to evaluate cross sections of inelastic scattering from the molybdenum isotopes.

KEYWORDS: DWBA, coupled-channels, statistical model, molybdenum, neutron, inelastic scattering, cross sections, fission products

I. INTRODUCTION

Recent integral tests[1][2][3] of fission product (FP) nuclear data and their analyses[4] showed a requirement of accurate cross sections for neutron inelastic scattering[5]. A neutron energy range of interest for a nuclear reactor design is below about 10 MeV, and two dominant nuclear reaction processes contribute to the inelastic scattering in this energy range, *i.e.*, the direct process and the compound process. It is known that many nuclei in the FP mass range have characteristics of collective excitation, and the direct process should be taken into account for an evaluation of the FP nuclear data.

The direct process contribution to the inelastic scattering can be calculated with a distorted-wave Born approximation (DWBA) or with a coupled-channels (CC) theory, and the DWBA has been widely used for the nuclear data evaluation of JENDL-3[6][7] because it has a rather simple formulation, and it is regarded as a good approximation of the coupled-channels theory when nuclear deformation is small. However, anomalous enhancement of DWBA cross sections near the threshold of inelastic scattering has been reported[5][8] around $A \sim 100$ when global optical potential parameters were used.

This problem has been discussed in the subgroup 10 of International Evaluation Cooperation Working Party[9][10] organized under the Nuclear Energy Agency Nuclear Science Committee, but the reason for

*6-1 Kasuga-kouen, Kasuga 816-8580, Japan
**1-1 Oho, Tsukuba 305-0801, Japan

the enhancement has not been found yet, and it is often claimed[5] that the DWBA is inappropriate for the evaluation of the FP nuclear data. Therefore it is important to validate the DWBA calculation used in the existent nuclear data files.

Isotopes of molybdenum show typical collective excitation, and the properties of the low-lying states have been studied with Coulomb excitation and electron, proton scattering[11][12]. The studies indicated that the experimental data can be represented by a coupling of the ground state with the collective one-phonon state. Recent experimental data of the neutron inelastic scattering[13] from the molybdenum isotopes may be interpreted with the same coupling scheme, and comparisons of the DWBA calculations with the CC ones may provide the reason for the enhancement or the limitation of the DWBA.

In the analysis of the neutron inelastic scattering data, we need an appropriate neutron optical potential set and deformation parameters, as a reference compared with a global optical potential. Smith *et al.*[14] made the optical model analysis for the data of neutron induced reactions on nuclei with $Z = 39$–51, and they obtained the regional optical potential parameters from the differential elastic scattering and the total cross sections in the energy range of 1.5 to 4 MeV. This regional optical potential, as well as the deformation parameters obtained by the CC analyses of the proton-induced reaction data, provides a good basis for the comparison between the DWBA and CC calculations.

In the present paper we investigate the anomalous enhancement of the DWBA calculation with a global potential, and show the difference between the DWBA and the CC calculations for the molybdenum isotopes. Section II describes the DWBA calculation for ^{100}Mo. The enhancement of the DWBA cross sections near the threshold is examined and comparisons of the DWBA and CC calculations are made. Model calculations using the regional potential of Smith *et al.*[14] are compared with the experimental data of the inelastic scattering from molybdenum isotopes in Section III. Finally, Section IV summarizes conclusions.

II. Enhancement of DWBA Cross Sections

1. Calculations with Global Optical Potentials

The direct inelastic scattering cross sections are calculated for the low-lying 2^+ (535.6 keV) and 3^- (1908 keV) levels of ^{100}Mo. We assume these levels are one-phonon states, and the deformation parameters β_2 and β_3 are taken from proton scattering experiments[12]: $\beta_2 = 0.214$ and $\beta_3 = 0.208$. The global optical potential of Walter-Guss[15] (WG) and its modified set[16] are used in the DWBA calculation. The Walter-Guss optical potential was obtained from the experimental data above 20 MeV. Yamamuro[16] extrapolated the Walter-Guss potential below 20 MeV by changing the imaginary potential depth so as to reproduce experimental non-elastic cross sections in this energy range. The modified Walter-Guss potential has an imaginary surface term

$$W_s = \begin{cases} 7.21 & -14.94\varepsilon & & \text{MeV} & (E < 20\ \text{MeV}) \\ 10.85 & -14.94\varepsilon & -0.1571E & \text{MeV} & (E \geq 20\ \text{MeV}) \end{cases}, \tag{1}$$

where $\varepsilon = (N - Z)/A$, and E an incident neutron energy. The modified potential was used in the evaluation of the inelastic scattering cross section of Molybdenum isotopes for JENDL-3.2.

The DWBA cross sections for ^{100}Mo are calculated with the code CmC[17]. Coupled-channels calculation is carried out with the ECIS88 code[18], which solves coupled equations by a sequential iteration method, and its first iteration corresponds to the DWBA calculation.

The collective inelastic scattering cross sections for the 2^+ and the 3^- states are shown in Figs. 1 and 2, respectively. The cross sections with the CC theory are shown in the same figures by the dot-dashed lines. The optical potential for the CC calculation is the same as that for the DWBA calculation. One can obviously see the anomalous enhancement of the cross sections near the threshold energy when the modified Walter-Guss potential is used. This enhancement does not come from a problem of the code, because the DWBA calculations with ECIS88 are almost the same as those obtained with CmC. The

enhancement appears in the CC result too, but it is more moderate than that with the DWBA. In the case of the original Walter-Guss potential, there is no enhancement in the both calculations with DWBA and CC. It is known[19] that the unitarity, $|S_{ba}| \leq 1$, is not necessary for a scattering matrix calculated by the DWBA, but the CC method ensures it. The demands of unitarity partly suppress the anomalous enhancement in the inelastic channel. However, the excitation function of the cross sections is rather steep just above the threshold energy. Therefore, even the CC theory yields large cross sections by using the modified Walter-Guss potential.

The enhancement of the inelastic scattering cross sections only appears when the modified Walter-Guss potential is used, and one can conclude that the enhancement is due to the optical potential used. In order to examine the difference in the original Walter-Guss potential and the modified one, we compare the distorted-waves. As seen in Fig. 1, a sudden rise of the cross section occurs just above the threshold energy. It means that the anomaly is related to the distorted-waves at several hundreds keV. The squared radial wavefunctions at a neutron energy E_n of 100 keV are shown in Fig. 3, where the nuclear radius is 5.57 fm. Strong absorption of the p-wave is shown for the modified Walter-Guss potential. The spin-averaged transmission coefficients T_l at 0.1 MeV are 0.158 for the original potential and 0.229 for the modified one.

A size resonance for a $3p$-wave is observed[20] for $A \sim 100$. The s-wave and p-wave strength functions for those optical potentials are tabulated in Table 1. The strength functions with the spherical optical potential by Smith *et al.*[14] are also given in this table, because they paid attention to the strength functions as well as the cross sections in the analyses. It is found from the table that the original Walter-Guss potential gives the strength functions almost consistent with those of Mughabghab[20], while the modified Walter-Guss potential gives a larger p-wave strength function. The strength functions with the optical potential by Smith *et al.* are in good accordance with the Mughabghab's values, and the calculated DWBA cross section does not show the anomalous enhancement. For example, the DWBA cross section for the 2^+ state at $E_n = 3$ MeV is 117 mb, and this value is, as seen in Fig. 1, near to the DWBA or CC results calculated with the original Walter-Guss potential.

An increase in the p-wave amplitude enhances the DWBA calculation. A DWBA transition amplitude is proportional to a radial overlap integral[19] between the initial and the final states:

$$I_{ba}^{L} = \frac{\sqrt{4\pi}}{k_a k_b} \int u_b(r) F_L(r) u_a(r) dr, \tag{2}$$

where $u_a(r)$ and $u_b(r)$ are the radial part of distorted-waves, L is the orbital angular momentum transfer, and $F_L(r)$ is the form factor. The DWBA cross section is calculated from the squared transition amplitudes, and it is possible to see the contribution to the DWBA calculation from various partial waves if one compares the overlap integrals. Figure 4 shows the squared overlap integrals as a function of the radius,

$$|I(r)|^2 = \left| \int_0^r u_b(r') F_L(r') u_a(r') dr' \right|^2 . \tag{3}$$

The distorted-waves in Fig. 4 are both for p-wave (the total spin is $j_a = j_b = 3/2$), and L transfer is 2. We assume the excitation energy of the 2^+ state is zero in order to equate the distorted-waves for the entrance and the exit channels. The overlap integral with the modified Walter-Guss potential is very large in comparison with the case of the original potential. This enhancement also appears in the overlap integral between the p-wave and f-wave, and the strong contribution from the p-wave results in the anomalous enhancement of the DWBA cross section. This enhancement becomes smaller as the incident neutron energy increases, because many partial waves contribute to the total inelastic scattering cross sections, and the relative importance of the p-wave reduces.

2. Calculations with Simplified Optical Potentials

The difference between the original Walter-Guss potential and the modified one for ^{100}Mo is the depth of the imaginary potential W_s: $W_s = 8.46$ MeV with the original potential and $W_s = 5.32$ MeV with the

modified one at $E_n = 0$. Figure 5 shows the dependence of the imaginary part of the S matrix element for p-wave on W_s at $E_n = 1$ keV. As W_s decreases the imaginary part of the S matrix element increases and it becomes positive at ~ 3 MeV for $j = 3/2$ and at ~ 6 MeV for $j = 1/2$. The calculated DWBA cross sections for the 2^+ level at $E_n = 1$ MeV are depicted in the same figure by the dot-dashed line. One can see the relation between the DWBA cross section and the imaginary part of the S matrix element. When a spherical optical model calculation gives $\mathrm{Im}(S_1) > 0$ at $E_n \to 0$, the calculated DWBA cross section becomes very large. For example, both $\mathrm{Im}(S_1^{3/2})$ and $\mathrm{Im}(S_1^{1/2})$ are positive below $W_s = 3$ MeV, and the DWBA cross sections are unacceptably large there.

In order to investigate the dependence of the DWBA cross section on the p-wave S matrix element, we employ a simplified optical potential:

$$\begin{aligned} V &= 50 \text{ MeV}, \quad r_v = 1.2 \text{ fm}, \quad a_v = 0.6 \text{ fm}, \\ W_s &= 3 \text{ or } 5 \text{ MeV} \quad r_w = 1.3 \text{ fm}, \quad a_w = 0.6 \text{ fm}, \end{aligned} \tag{4}$$

without a spin-orbit term. This optical potential gives $\mathrm{Im}(S_1) > 0$ for $W_s = 3$ MeV, and $\mathrm{Im}(S_1) < 0$ for $W_s = 5$ MeV. The inelastic scattering cross sections for the 2^+ level of ^{100}Mo whose excitation energy is set to zero are calculated with the DWBA, and the level excitation function is shown in Fig. 6, being compared with the partial cross sections of the spherical optical model (SOM),

$$\sigma_T^\ell = \frac{2\pi}{k^2}(2\ell+1)\{1 - \mathrm{Re}(S_\ell)\}. \tag{5}$$

Two resonance-like peaks of the DWBA cross section appear when $W_s = 3$ MeV, while in the case of $W_s = 5$ MeV the enhancement of the DWBA cross section is small. It is found from Fig. 6 that the first peak near $E_n = 500$ keV corresponds to the p-wave contribution, and the second one near 2 MeV is from f-wave.

This anomalous enhancement may occur in the mass region where the s-wave strength function takes the maxima. The $3s$ size resonance appears around $A \sim 50$. The imaginary part of the s-wave S matrix element becomes positive when the following optical potential is used.

$$\begin{aligned} V &= 52 \text{ MeV}, \quad r_v = 1.2 \text{ fm}, \quad a_v = 0.6 \text{ fm}, \\ W_s &= 1 \text{ MeV}, \quad r_w = 1.3 \text{ fm}, \quad a_w = 0.6 \text{ fm}. \end{aligned} \tag{6}$$

The calculated DWBA cross sections for ^{50}Cr are shown in Fig. 7. The anomalous enhancement of the DWBA occurs near $E_n = 2.5$ MeV and 4.5 MeV, and the two peaks are corresponding to the d-wave and g-wave contributions, respectively. The imaginary part of the optical potential in Eq. (6) is unphysically shallow. If one increases the imaginary depth to 3 MeV, the anomalous enhancement disappears as indicated by the thin solid line in Fig. 7.

It is found from Figs. 6 and 7 that the anomaly happens when the imaginary potential is very shallow. Some global optical potentials have a symmetry term $(N-Z)/A \times W_{sym.}$, and the Walter-Guss optical potential contains the term $-14.94(N-Z)/A$ MeV in the surface imaginary part. Thus, the imaginary part becomes small for a nucleus which has excessive neutrons. Table 2 shows the calculated DWBA cross sections with the original Walter-Guss optical potential[15] and with the modified one[16], at $E_n = 1$ MeV for some stable isotopes — ^{40,48}Ca, ^{78,86}Kr, ^{102,110}Pd, and ^{156,164}Dy. The calculated cross sections are for the collective excited states with $J^\pi = 2^+$ and $\beta_2 = 0.1$, and the excitation energies are assumed to be zero. The enhancement is observed when the modified Walter-Guss potential is used, and the effect is larger for the heavy nuclei.

III. Comparison with Experimental Data

Measurements of the $(n, n'\gamma)$ reaction cross sections for Mo isotopes were made at IRMM[13] (Commission of the European Communities, Joint Research Centre, Institute for Reference Materials and Measurements). To analyze the experimental data we employ the DWBA and CC methods for the collective

direct process, and the Hauser-Feshbach-Moldauer model for the compound process. As was mentioned in Section II, the modified Walter-Guss potential is inadequate to calculate the direct cross sections at low energies, while the optical potential by Smith *et al.*[14] is appropriate because their potential gives a p-wave strength function which is in good agreement with experimental data, and the potential is defined in the energy range $E_n \lesssim 5$ MeV which covers the energy range where the experimental data exist.

The experimental inelastic scattering data were obtained by means of the γ-ray detection[13]. The experimental data for the 535.6 keV level of ^{100}Mo are not resolved, and they contain the cross section to the first excited state (535.6 keV) and 88% of that to the second excited state (695.1 keV). The excited level of 535.6 keV is a one-phonon 2^+ state, and the 695.12 keV level is a member of the two-phonon triplet, 0^+(695.1 keV), 2^+(1064 keV), and 4^+(1136 keV). Since the cross sections for the two-phonon triplet are expected to be small, the direct inelastic scattering cross sections are calculated only for the one-phonon states (2^+ and 3^-). The deformation parameters are $\beta_2 = 0.214$ and $\beta_3 = 0.208$[12].

The compound cross sections are calculated with the Hauser-Feshbach theory with the width fluctuation correction by Moldauer[21]. The discrete levels up to an excitation energy of 2.3 MeV are included in the calculation, and their J^π values are taken from ENSDF[22]. The excited levels are assumed to be overlapped above 2.3 MeV, and Gilbert and Cameron's formulas[23] are used to calculate the level density in the continuum region. The level density parameters are taken from the code EGNASH[16] built-in values, and the adopted level density parameters in the Fermi gas model are $a = 17.9$ MeV^{-1} and $\Delta = 2.22$ MeV. At low excitation energies, the constant temperature model is used, and its parameters are determined by a, Δ, and the discrete levels.

A comparison of the calculated cross sections with the experimental data is shown in Fig. 8. The thick solid line is an incoherent sum of the DWBA calculation and the Hauser-Feshbach-Moldauer calculation for the 535.6 keV level including the 88% of the 695.1 keV level. The thin solid line is the compound cross sections for the 1064 keV level. The calculated cross sections for the 1064 keV level are in good agreement with the measurements, while the calculations for the 535.6 keV level are overestimated. There are some possible reasons, those are, the deformation parameters, the width fluctuation correction, and the difference between DWBA and CC calculations.

The deformation parameters are taken from the (p,p') experiment[12]. It is possible to correct the β's for neutron induced reactions if one applies the relation $\beta_p R_p = \beta_n R_n$, where R_n and R_p are the nuclear radii for the neutron and proton scattering, and they are $\beta_2 = 0.205$ and $\beta_3 = 0.199$ when R_n of Smith *et al.*[14] is used. This correction reduces the cross sections for the first level slightly: 0.7% at 1.5 MeV.

In order to calculate the width fluctuation correction factor, it is necessary to know the distribution of level widths in the compound nucleus, and a χ^2-distribution with ν degrees of freedom is assumed. Moldauer[21] obtained a practical expression for ν by a Monte Calro method, which is adopted in this study. The other assumption is $\nu = 1$, which means the distribution is the Porter-Thomas distribution. The calculated cross sections with $\nu = 1$ are shown in Fig. 8 by the dot-dashed lines. The compound cross sections decrease and the level excitation function becomes very similar to the experimental data.

The coupled-channels calculations were made for the 0^+-2^+-3^- coupling scheme with ECIS88, and the results are compared with the experimental data in Fig. 9. The thick dotted line is the direct component, and the thick solid line is the sum of the direct and the compound cross sections. The calculated cross sections are very similar to those with the DWBA in Fig. 8, and it can be concluded that the DWBA is a useful tool for an evaluation of the direct process as long as the optical potential is adequate.

The calculated cross section for the 535.6 keV level can be compared with some neutron measurements[24][25][26][27] and the comparison is shown in Fig. 10. The calculation reproduces the tendency of the experimental data, although the data are scattered. The evaluated cross section in JENDL-3.2 which used DWBA calculations with the modified Walter-Guss potential is shown in the same figure by the dashed line.

Comparisons of the ^{98}Mo inelastic scattering data with the DWBA and the compound calculations are shown in Fig. 11. The discrete levels up to 2.57 MeV were included, and the level density parameters of $a = 15.8$ MeV^{-1} and $\Delta = 2.57$ MeV were used[16]. We regarded the 787.4 keV level ($J^\pi = 2^+$) as

a collective one-phonon state. The deformation parameter employed is $\beta_2 = 0.162$[12]. The excitation function of the 734.8 keV level ($J^\pi = 0^+$) is depicted by the dashed line, but it cannot be measured by a γ-ray detection because a γ-ray transition between the same spin-parity states is prohibited by the selection rule. The cross sections for the second (787.4 keV) and the third (1432 keV) levels are well reproduced by the sum of the DWBA and the compound cross sections.

Figure 12 illustrates the calculated cross sections for the ^{92}Mo inelastic scattering. The discrete levels included in the compound process calculation are below 3.69 MeV, and $a = 10.6$ MeV^{-1} and $\Delta = 2.21$ MeV were used[16] in the continuum. The DWBA calculations for the collective state of 1509 keV ($J^\pi = 2^+$) were made with $\beta_2 = 0.101$[12]. The calculated cross sections exceed the experimental data above 2 MeV. The overestimation is essentially a problem of the compound calculation because the DWBA cross sections are very small in this energy range. The compound cross section for the 1509 keV level at $E_n = 2$ MeV is 886 mb, and if $\nu = 1$ for the width fluctuation correction is assumed the cross section becomes 752 mb, which agrees with the experimental data.

IV. Conclusion

Anomalous enhancement of the DWBA cross sections for ^{100}Mo near the threshold energy appears when the optical potential has a small imaginary part. The enhancement tends to occur when global optical potentials with a symmetry term in the imaginary part are used for nuclei which have excessive neutrons. The problem is seen in the coupled-channels calculation too, although the magnitude of the enhancement is smaller.

The enhancement of the DWBA calculation can be attributed to a large p-wave amplitude. An optical potential which yields too large p-wave strength function tends to give a large DWBA cross section. When the DWBA cross sections are physically reasonable, the differences between the DWBA and the coupled-channels are small.

The DWBA and the Hauser-Feshbach-Moldauer calculations with the spherical optical potential by Smith *et al.* give the inelastic scattering cross sections in the energy range $E_n \lesssim 5$ MeV, which are in good agreement with the recent experimental data at IRMM. A method of the width fluctuation correction is sensitive to the compound cross section calculation in this energy range.

Applicability of the DWBA method to the FP nuclear data evaluation has been argued since the anomalous enhancement of the cross sections were reported. This problem can be avoided if one adopts an adequate optical potential, and it can be concluded that the DWBA method is a useful tool to evaluate the FP nuclear data.

Acknowledgment

We are indebted to Dr. F. H. Fröhner for his valuable discussion. We are grateful to Dr. H. Weigmann in IRMM for providing the numerical experimental data. We thank the members of the Evaluation, Calculation System Working Group in Japanese Nuclear Data Committee for their useful comments.

— References —

(1) Veenema, J. J., Janssen, A. J. : *ECN* 10 (1976).

(2) Janssen, A. J., Gruppelaar, H., Karouby-Cohen, N., Martin-Deidier, L., Rimpault, G., Salvatores, M. : *ECN* 176 (1985).

(3) Watanabe, T., Kawai, M., Zukeran, A., Matsunobu, H., Nakagawa, T., Nakajima, Y., Sugi, T., Chiba, S., Sasaki, M. : *Proc. Specialists' Meeting on Fission Product Nuclear Data, Tokai, Japan, 25-27 May 1992*, p.411 (1992).

(4) Gruppelaar, H., van der Kamp, H. A. J. : *Proc. Specialists' Meeting on the Use of the Optical Model for the Calculation of Neutron Cross Sections Below 20 MeV, Paris, France, 13-15 Nov. 1985*, p.221 (1986).

(5) Gruppelaar, H., Hogenbirk, A. : *Proc. Specialists' Meeting on Fission Product Nuclear Data, Tokai, Japan, 25-27 May 1992*, p.207 (1992).

(6) Kawai, M., Iijima, S., Nakagawa, T., Nakajima, Y., Sugi, T., Watanabe, T., Matsunobu, H., Sasaki, M., Zukeran, A. : *J. Nucl. Sci. Technol.*, **29**, 195 (1992).

(7) Kawai, M., Zukeran, A., Nakagawa, T., Chiba, S., Nakajima, Y., Sugi, T., Kikuchi, Y., Watanabe, T., Matsunobu, H. : *Proc. Int. Conf. Nuclear Data for Science and Technology, Gatlinburg, U.S.A., 9-13 May 1994*, p.727 (1994).

(8) Chiba, S., Smith, A. B. : *Proc. Specialists' Meeting on Fission Product Nuclear Data, Tokai, Japan, 25-27 May 1992*, p.162 (1992).

(9) Kawai, M., Gruppelaar, H., Schenter, R. E., Wright, R. Q. : *Proc. Specialists' Meeting on Fission Product Nuclear Data, Tokai, Japan, 25-27 May 1992*, p.39 (1992).

(10) Kawai, M., Chiba, S., Nakagawa, T., Nakajima, Y., Watanabe, T., Zukeran, A., Gruppelaar, H., Hogenbirk, A., Salvatores, M., Dietze, K., Wright, R. Q., Schenter, R. E. : *Proc. Int. Conf. Nuclear Data for Science and Technology, Gatlinburg, U.S.A., 9-13 May 1994*, p.795 (1994).

(11) Lutz, H. F., Heikkinen, D. W., Bartolini, W. : *Phys. Rev.*, **C4**, 934 (1971).

(12) Cereda, E., Pignanelli, M., Micheletti, S., von Geramb, H. V., Harakeh, M. N., De Leo, R., D'Erasmo, G., Pantaleo, A. : *Phys. Rev.*, **C26**, 1941 (1982).

(13) Birn, I. -G., Meister, A., Wattecamps, E., Weigmann, H. : *Proc. Int. Conf. Nuclear Data for Science and Technology, Trieste, Italy, 19-24 May 1997, to be published*, Numerical data by private communication.

(14) Smith, A. B., Guenther, P. T., Whalen, J. F. : *Nucl. Phys.*, **A415**, 1 (1984).

(15) Walter, R. L., Guss, P. P. : *Proc. Int. Conf. Nuclear Data for Basic and Applied Science, Santa Fe, 13-17 May, 1985*, p.1079 (1986), *Rad. Effect*, **95**, 73 (1986).

(16) Yamamuro, N. : *JAERI-M* 90-006 (1990).

(17) Kawano, T. : "*program CmC*", unpublished.

(18) Raynal, J. : "*program ECIS88*", unpublished.

(19) Satchler, G. R. : "*Direct Nuclear Reactions*", Oxford Press (1983).

(20) Mughabghab, S. F., Divadeenam, M., Holden, N. E. : "*Neutron Cross sections*" Vol.1: "*Neutron Resonance Parameters and Thermal Cross Sections*", Academic Press, New York (1981).

(21) Moldauer, P. A. : *Nucl. Phys.*, **A344**, 185 (1980).

(22) National Nuclear Data Center (BNL) : "*Evaluated Nuclear Structure Data File, ENSDF*".

(23) Gilbert, A., Cameron, A. G. W. : *Can. J. Phys.*, **43**, 1446 (1965).

(24) Lambropoulos, P., Guenther, P., Smith, A., Whalen, J. : *Nucl. Phys.*, **A201**, 1 (1973).

(25) McEllistrem, M. T., Brandenberger, J. D., Sinram, K., Glasgow, G. P., Chung, K. C. : *Phys. Rev.*, **C9**, 670 (1974).

(26) McDaniel, F. D., Brandenberger, J. D., Glasgow, G. P., Leighton, H. G. : *Phys. Rev.*, **C10**, 1087 (1974).

(27) Smith, A. B., Guenther, P., Whalen, J. : *Nucl. Phys.*, **A244**, 213 (1975).

Table 1: s-wave and p-wave strength functions for ^{100}Mo.

	s-wave $\times 10^4$	p-wave $\times 10^4$
Mughabghab *et al.*	0.73 ±0.17	4.4 ±0.9
original WG	0.91	5.1
modified WG	0.61	7.5
Smith *et al.*	0.75	4.9

Table 2: Calculated DWBA cross sections with the original Walter-Guss potential and the modified Walter-Guss potential. The values of W_s are at $E_n = 0$ MeV. The DWBA cross sections are for the collective 2^+ states at $E_n = 1$ MeV, assuming $\beta_2 = 0.1$ and the excitation energy of zero.

	$(N-Z)/A$	original WG		modified WG	
		W_s [MeV]	DWBA [mb]	W_s [MeV]	DWBA [mb]
^{40}Ca	0.0	10.85	4.882	7.710	8.647
^{48}Ca	0.167	8.360	11.73	5.220	27.20
^{78}Kr	0.0769	9.701	21.56	6.561	43.39
^{86}Kr	0.163	8.418	32.28	5.278	78.71
^{102}Pd	0.0980	9.385	17.57	6.245	43.62
^{110}Pd	0.164	8.405	20.76	5.265	51.28
^{156}Dy	0.154	8.552	51.94	5.412	174.4
^{164}Dy	0.195	7.935	57.45	4.795	213.1

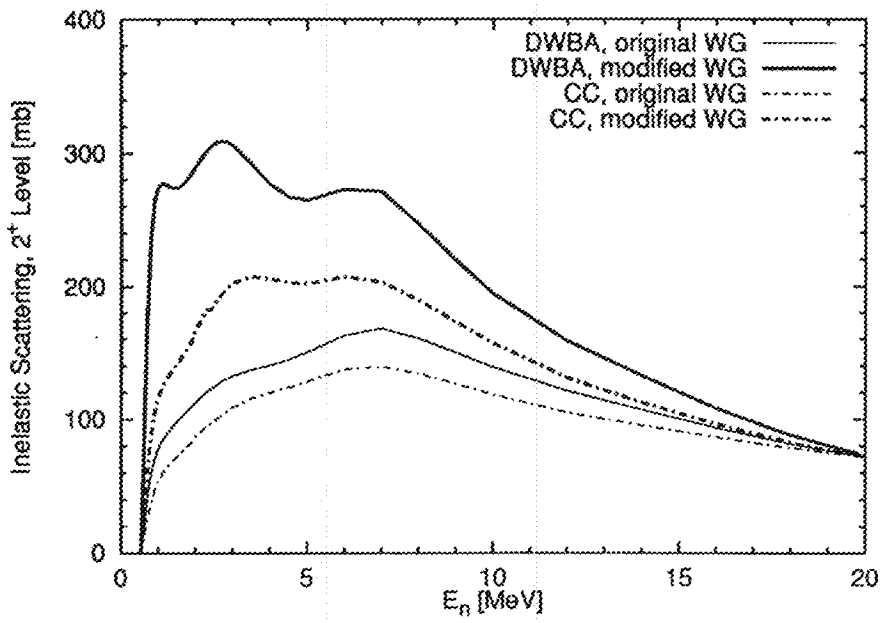

Fig. 1: Direct inelastic scattering cross sections to the 2^+ level calculated with the original Walter-Guss potential (thin lines) and the modified Walter-Guss potential (thick lines). The dot-dashed lines are the CC results with the 0^+-2^+-3^- coupling scheme.

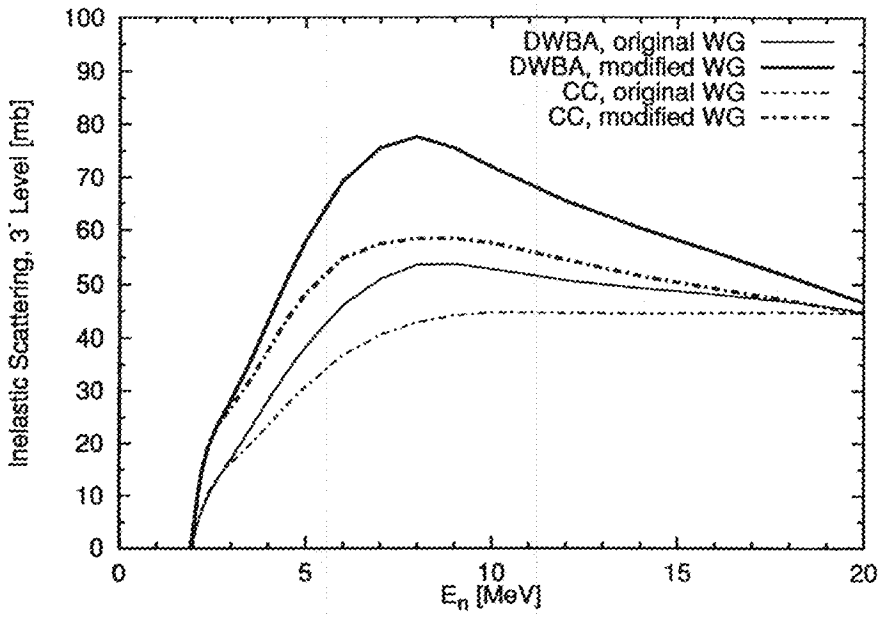

Fig. 2: Direct inelastic scattering cross sections to the 3^- level calculated with the original Walter-Guss potential (thin lines) and the modified Walter-Guss potential (thick lines). The dot-dashed lines are the CC results with the 0^+-2^+-3^- coupling scheme.

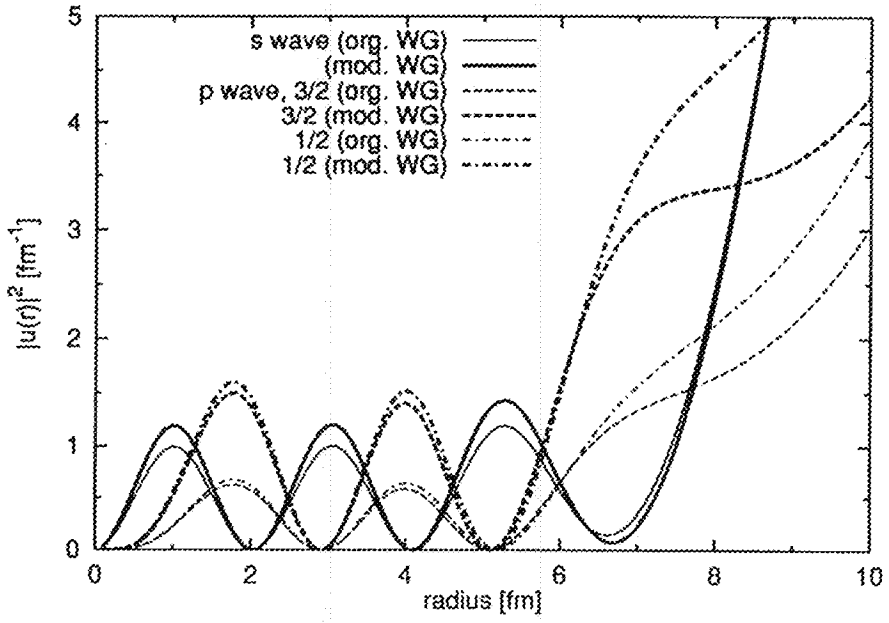

Fig. 3: The squared values of the radial wave functions at $E_n = 0.1$ MeV. The thin lines are calculated with the original Walter-Guss potential, and the thick lines are with the modified one.

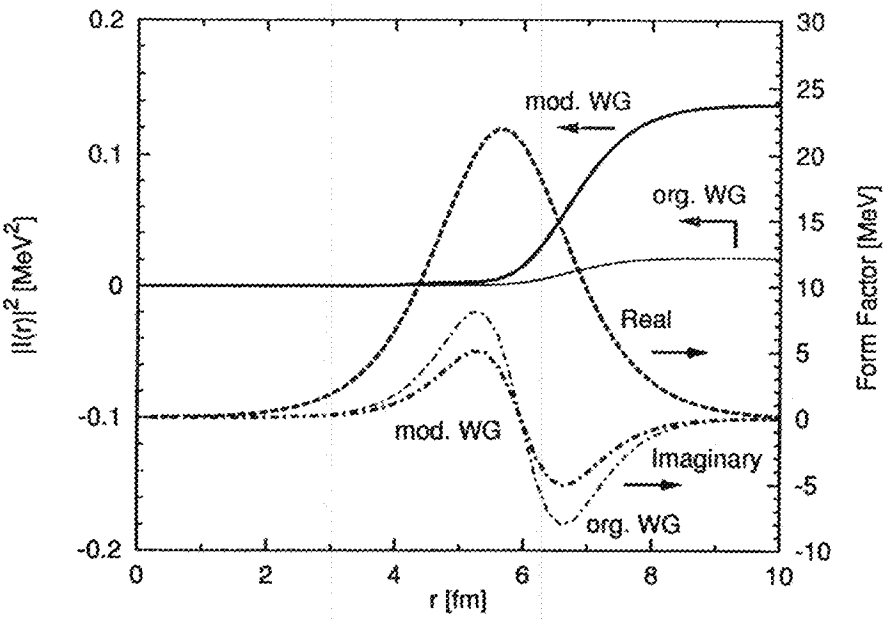

Fig. 4: Comparison of the overlap integral with the original Walter-Guss and the modified Walter-Guss potentials. The entrance channel and the exit channel wave functions are for the p-wave, $j = 3/2$ at $E_n = 0.1$ MeV. The collective form factor is shown by the dashed line (real) and the dot-dashed lines (imaginary). The real parts of both potentials are the same.

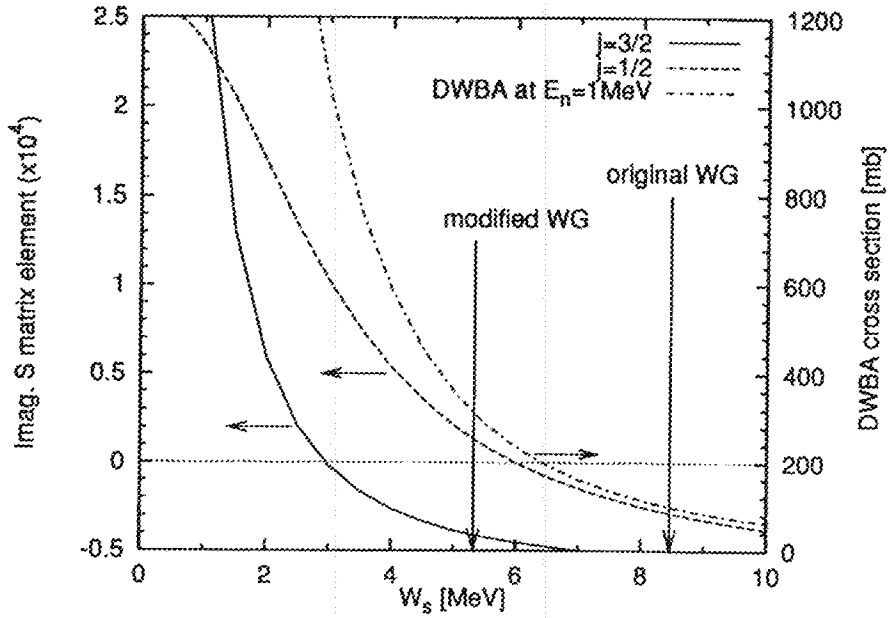

Fig. 5: Imaginary part of S matrix elements at $E_n = 1$ keV, and DWBA cross sections at $E_n = 1.0$ MeV, as a function of depth of the imaginary potential, W_s.

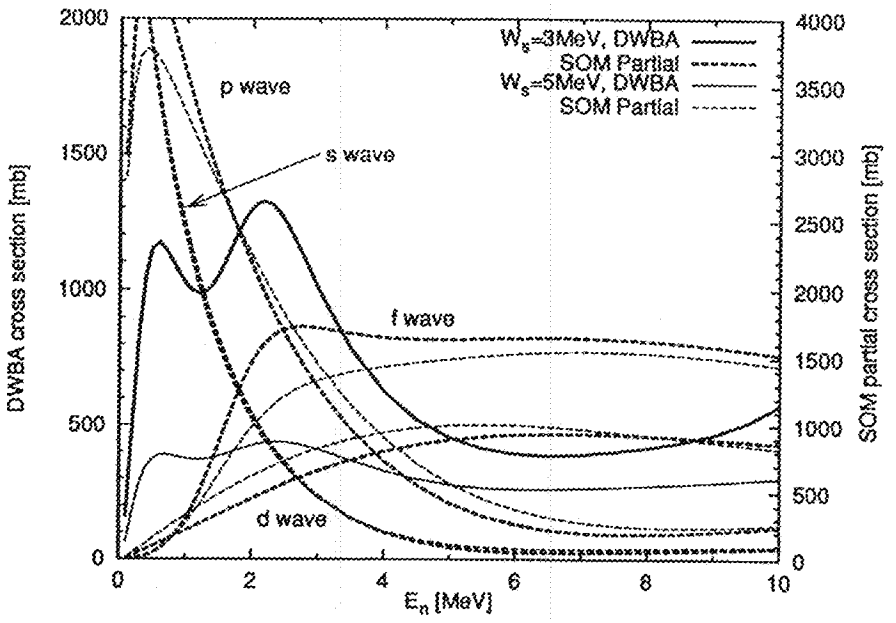

Fig. 6: Comparison of the calculated DWBA cross sections for ^{100}Mo and the partial cross sections (dashed lines). The DWBA cross sections are calculated for a ficticious level having the excitation energy of 0 MeV and the angular momentum transfer of $2\hbar$.

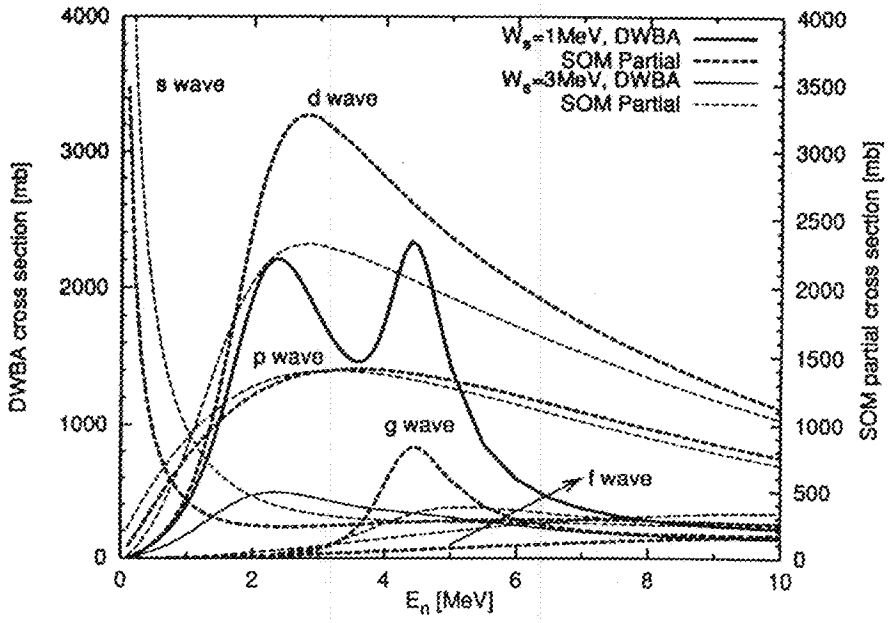

Fig. 7: Comparison of the calculated DWBA cross sections for ^{50}Cr and the partial cross sections (dashed lines). The DWBA cross sections are calculated for a ficticious level having the excitation energy of 0 MeV and the angular momentum transfer of $2\hbar$.

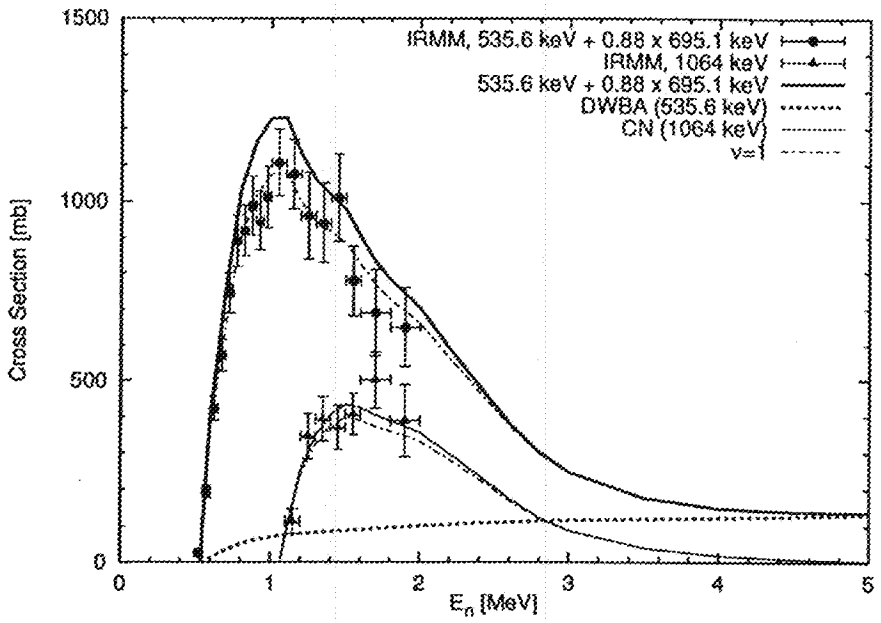

Fig. 8: Comparison of the calculated inelastic scattering cross sections of ^{100}Mo for the 535.6, 695.1, and 1064 keV levels with the experimental data. Cross sections for the first level contain 88% of the second level. The direct process is calculated with the DWBA. Cross sections for the 1064 keV level contain the compound nucleus (CN) process only. The dot-dashed line corresponds to the compound cross section calculated on the assumption that the level widths distribution is the Porter-Thomas distribution.

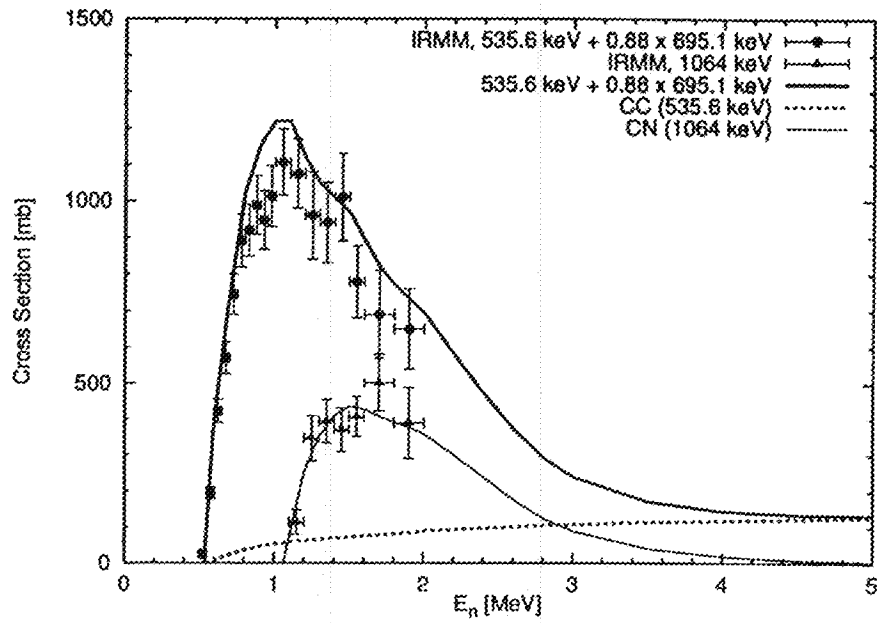

Fig. 9: Same as Fig. 8, but the direct process is calculated with the CC.

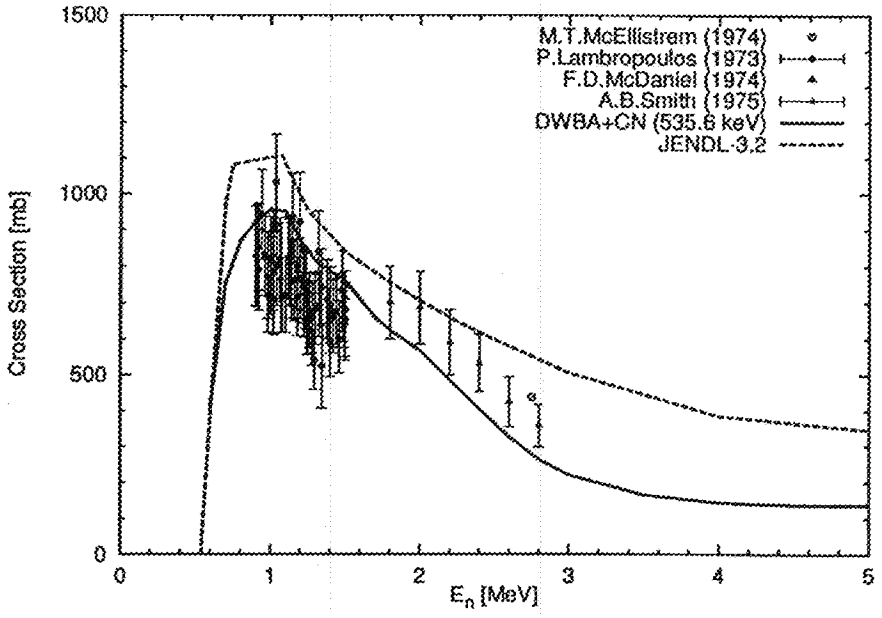

Fig. 10: Comparison of the calculated inelastic scattering cross sections of ^{100}Mo for the 535.6 keV level with the experimental data.

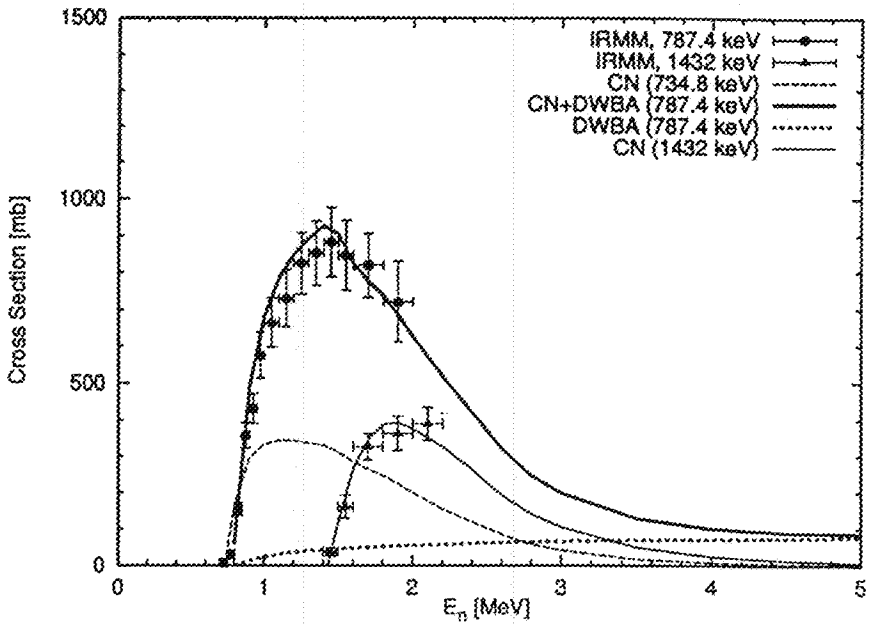

Fig. 11: Comparison of the calculated inelastic scattering cross sections of ^{98}Mo for the 787.4, and 1432 keV levels with the experimental data, as well as the calculated cross sections for 734.8 keV level.

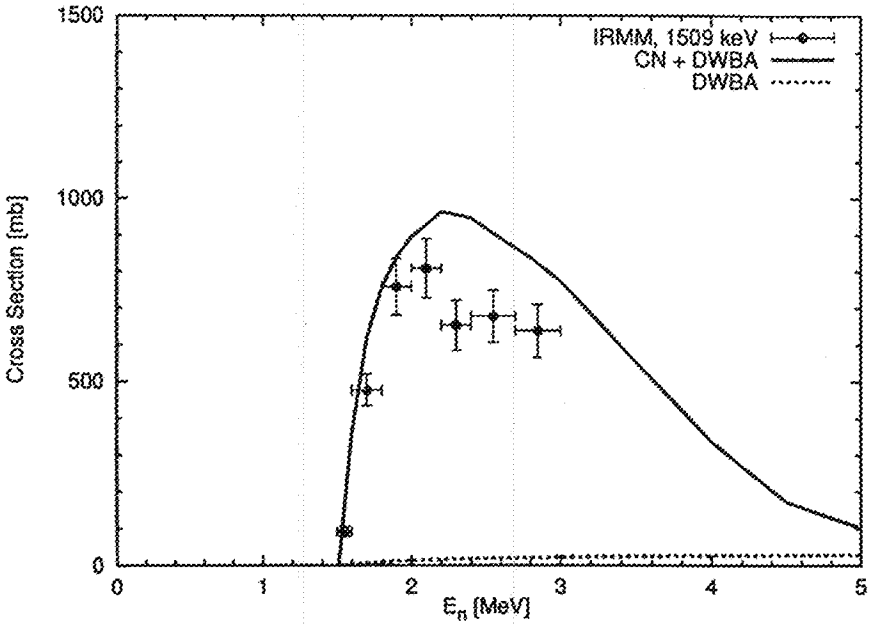

Fig. 12: Comparison of the calculated inelastic scattering cross sections of ^{92}Mo for the 1509 keV level with the experimental data.